



ELSEVIER

The dynamics and energetics of water permeation and proton exclusion in aquaporins

Bert L de Groot¹ and Helmut Grubmüller²

Aquaporins and aquaglyceroporins are passive membrane channels that, in many species, facilitate highly efficient yet strictly selective permeation of water and small solutes across lipid bilayers. Their ability to block proton flux is particularly remarkable, because other aqueous pores and water efficiently conduct protons, via the so-called Grotthuss mechanism. How efficient water permeation is achieved and how it is reconciled with the seemingly contradictory task of strict proton exclusion have been long-standing puzzles. Because neither the dynamics of the water molecules nor the mobility of protons inside the aquaporin channel could be experimentally accessed so far, several groups addressed this challenge using a variety of atomistic computer simulation methods.

Addresses

¹ Computational Biomolecular Dynamics Group, Max-Planck-Institute for Biophysical Chemistry, Am Fassberg 11, 37077 Göttingen, Germany

² Theoretical and Computational Biophysics Department, Max-Planck-Institute for Biophysical Chemistry, Am Fassberg 11, 37077 Göttingen, Germany

Corresponding author: Grubmüller, Helmut (hgrubmu@gwdg.de)

Current Opinion in Structural Biology 2005, **15**:176–183

This review comes from a themed issue on
Theory and simulation

Edited by J Andrew McCammon and Rebecca C Wade

Available online 5th March 2005

0959-440X/\$ – see front matter

© 2005 Elsevier Ltd. All rights reserved.

DOI 10.1016/j.sbi.2005.02.003

Introduction

Aquaporins are ubiquitous, highly specialized water channels in biological membranes [1,2]. Cell membranes are composed of lipid bilayers and thus are nearly impermeable to water. Yet many processes critically depend on the efficient exchange of water between the cell and its environment. Aquaporins enable passive yet remarkably efficient permeation of water molecules across cellular membranes in all tissues for which water balance is crucial, including the kidney, lung, brain, eye lens, skin and red blood cells. More than 350 aquaporins are known today; in humans alone, more than ten different aquaporins have been isolated so far with specialized permeation characteristics [3]. Their physiological relevance is further underscored by the fact that several diseases are associated with defective aquaporin functionality [4], including nephrogenic diabetes insipidus (aquaporin-2)

and congenital cataract (aquaporin-0). Aquaporins have been divided into two classes. The first primarily comprises strict water channels; members of the second class, also termed aquaglyceroporins, additionally conduct glycerol and other small solutes.

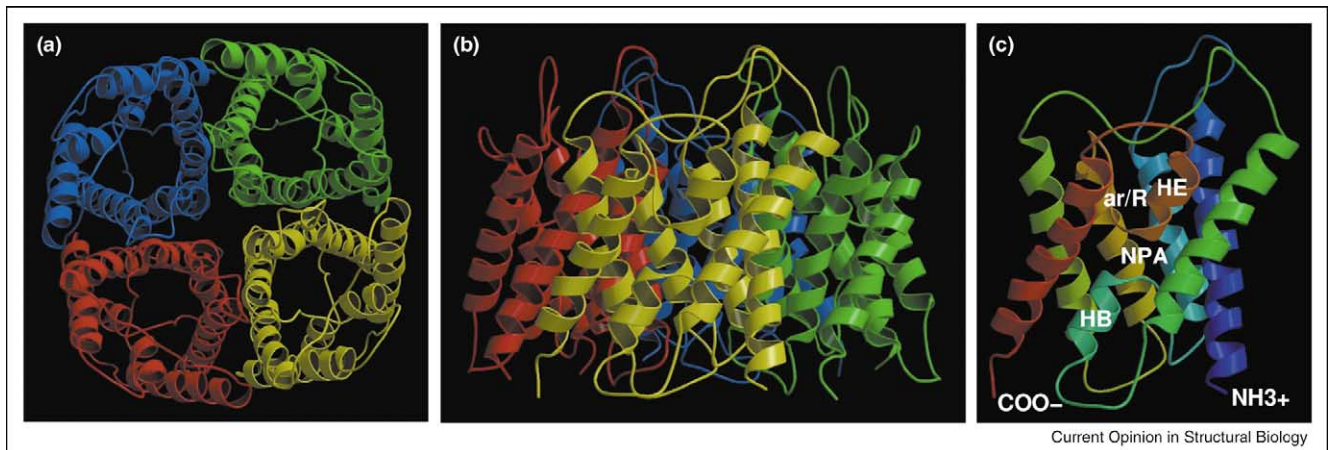
In virtually all organisms, proton gradients across cellular and subcellular membranes act as the primary energy source for the synthesis of ATP [5]. Maintaining the electrochemical gradient is, therefore, as crucial as efficient water permeation. In particular, it is essential that water flux through aquaporins is not accompanied by leakage of protons [6]. How these two apparently conflicting functions are reconciled has been a long-standing question in aquaporin research. The exclusion of protons is particularly intriguing against the background of high proton mobility in bulk water [7,8] and in other water-filled membrane proteins, such as gramicidin [9,10,11] and bacteriorhodopsin [12,13].

The elucidation of the first atomic structures of two different members of the aquaporin family [14,15] provided the basis for studying water permeation at an atomistic level and also prompted initial speculation on the mechanism of proton exclusion in terms of hydrogen bond interruptions [14]. These more structural aspects of aquaporin function have been extensively reviewed recently [16–19] and therefore are not discussed here. Figure 1 summarizes the main structural features of aquaporins. As the dynamics of water molecules and protons inside the pore are very fast and are not, so far, accessible to experiment, this issue has recently been addressed by several computer simulation studies using complementary methods. In close collaboration with experimental groups, this concerted effort has established from first principles the mechanisms of both efficient permeation of water (and glycerol) and strict selectivity against protons and other ions. The main results of these simulation studies and the emerging consensus mechanism are the focus of this review.

Mechanism of water permeation

High-resolution structures of aquaporin-1 (AQP1) [20,21] and the glycerol facilitator GlpF [15] enabled atomistic ‘real-time’ molecular dynamics (MD) simulations of spontaneous, full permeation events in aquaporins [22,23] (c.f. Figure 2a). It was found that both AQP1 and GlpF act as two-stage filters [22]. The first stage of the filter is located in the central part of the channel at the asparagine/proline/alanine (NPA) region; the second stage is located on the extracellular face of the

Figure 1



The structure of AQP1. All aquaporins and aquaglyceroporins of known structure are homotetramers consisting of four monomeric channels, as shown in (a) top view and (b) side view. The monomeric channel (c) displays internal pseudo-twofold symmetry, reflecting the sequence similarity of the N- and C-terminal halves of the molecule [24,25]. The channel consists of six transmembrane helices connected by five loops, termed A to E in AQP1. Loops A and D are short; loop C connects the two sequence-related halves of the molecule and spans the extracellular face of the channel. Loops B and E contain the highly conserved fingerprint NPA motifs, which fold back into the channel and meet at the channel center [14,24]. Both the B and E loops enter the channel as a loop and leave on the same side of the channel as a short helix. Located approximately 7 Å extracellular to the NPA region is the ar/R constriction region, the narrowest region of the pore. This constriction region is considerably narrower in water-specific AQP1 than in the glycerol facilitator GlpF.

channel in the aromatic/arginine (ar/R) constriction region. An independent simulation of GlpF [23^{••}], using a different force field, confirmed the crucial role of the NPA region; this had also been inferred from the fact that this motif is highly conserved [24,25]. These simulation studies also suggested mutants that changed the permeation characteristics in a predictable manner [23^{••}].

The simulations also addressed the energetics of water permeation. Overall, the channels achieve their high water permeability through a fine-tuned ‘choreography’ of hydrogen bonds [22^{••}]. Whenever and wherever bulk water–water hydrogen bonds have to be ruptured to allow the water molecule to ‘squeeze’ through the narrow NPA region, the protein offers ‘replacement’ interactions, which largely compensate for the energetic cost of water–water bond rupture. This remarkable complementarity to bulk water lowers the activation barrier to a large extent and thus allows the high permeation rate, which is observed both experimentally and in simulations, despite the hydrophobic nature of the pore. Further statistical analysis of the translational water dynamics revealed highly correlated motions, particularly within the NPA region, which additionally reduce the effective activation barrier to the experimentally determined value [22^{••}]. Protein–water interactions dominate only in the NPA and ar/R regions of the pore (c.f. Figure 2c). By contrast, water–water interactions dominate the energetics of water permeation in the other regions of the channel. The NPA region is characterized by two adjacent low hydrophobic free energy barriers, as has been revealed by

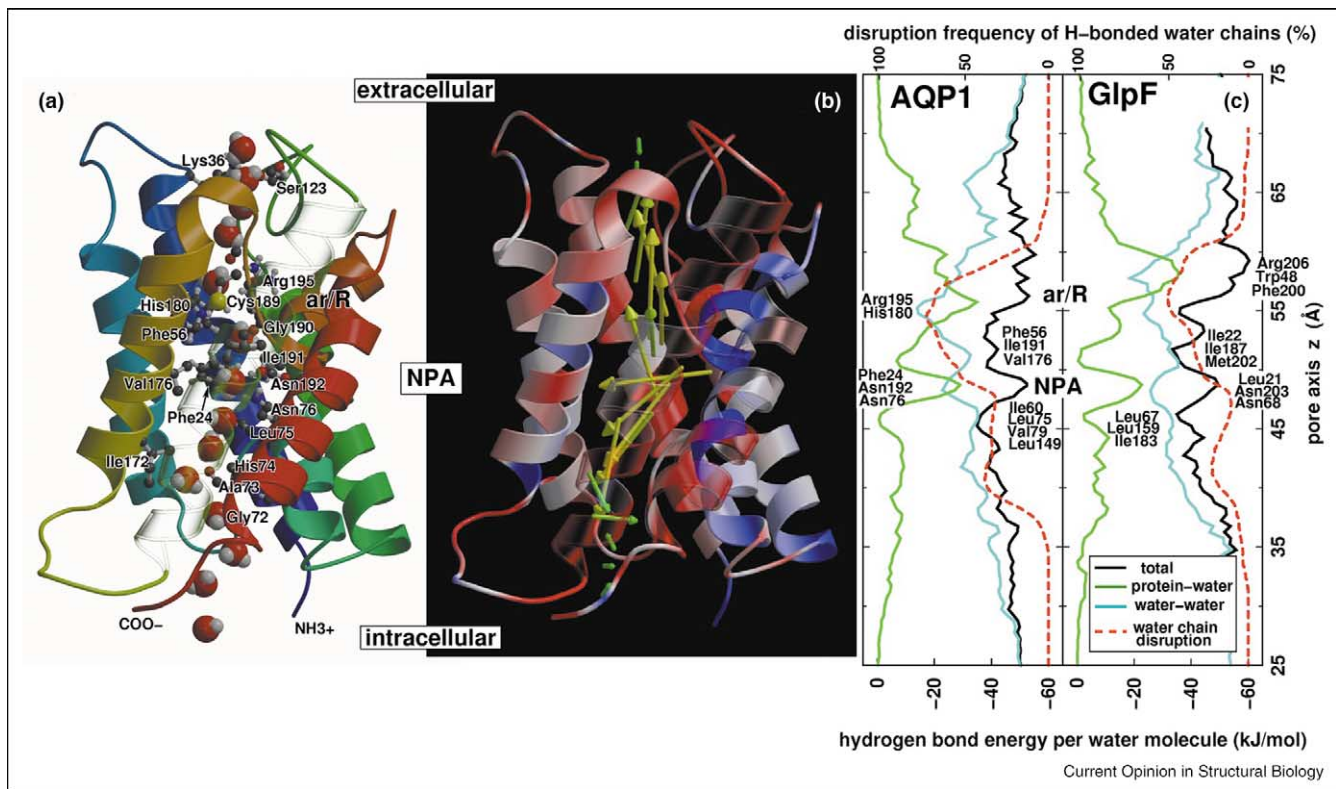
two independent computational approaches [22^{••},26]. The simulations finally revealed a pronounced water dipole orientation pattern across the channel, with the NPA region as its symmetry center [22^{••}]. In the simulations, the water molecules were found to rotate by 180° on their path through the pore (Figure 2b). The local electric field, which is dominated by the macrodipoles of helices B and E, has been suggested as the main cause [22^{••}].

This orientational distribution of water was subsequently and independently also observed for GlpF [23^{••}]. By artificially switching off the electric dipoles of the B and E helices in these simulations, it was convincingly and elegantly demonstrated that it is the electrostatic field generated by the helical macrodipoles that mainly determines the strict water dipole orientation [23^{••}]. By preventing the formation of a proton wire across the channel, this ‘global orientational tuning’ was proposed to block proton flux [23^{••},27].

Mechanism of glycerol permeation

Glycerol permeation through the bacterial glycerol facilitator GlpF has been observed to occur spontaneously [28] and has been systematically studied by applying external forces to the glycerol [29[•]]. Water and glycerol were found to move concertedly through the pore, thereby competing for hydrogen bond partners in the channel interior [28]. Employing Jarzynski’s equation, a potential of mean force for the permeation of glycerol through GlpF was derived from the force profiles of multiple force probe MD simulations [29[•]]. The minima

Figure 2



The mechanism of water permeation through AQP1 and GlpF [22^{**}]. **(a)** Typical pathway of a water molecule (red/white spheres) through the AQP1 pore. Residues lining the pore are labeled. **(b)** Orientational distribution of water dipoles within the pore. Arrows depict the mean dipoles of water molecules inside the pore. Because of the electrostatic field in the channel (color coded on the protein backbone), water molecules show a bipolar orientation within the pore, with the symmetry center located at the NPA region. **(c)** Hydrogen bond energetics of water molecules in the AQP1 and GlpF pores. Shown are water–water (blue), protein–water (green) and total mean hydrogen bond energies of water molecules, as well as the interruption frequency of water–water hydrogen bonds inside the AQP1 and GlpF pores (red).

in the free energy profile showed favorable qualitative agreement with the location of three glycerol molecules in the X-ray structure [15[•]]. Also, the stereoselectivity of the channel could be rationalized from these simulations [29[•]]. A broad free energy minimum was found at the periplasmic vestibule of the channel, which has been postulated to be involved in the recruitment of glycerol molecules, thereby enhancing the conduction rate [29[•],30].

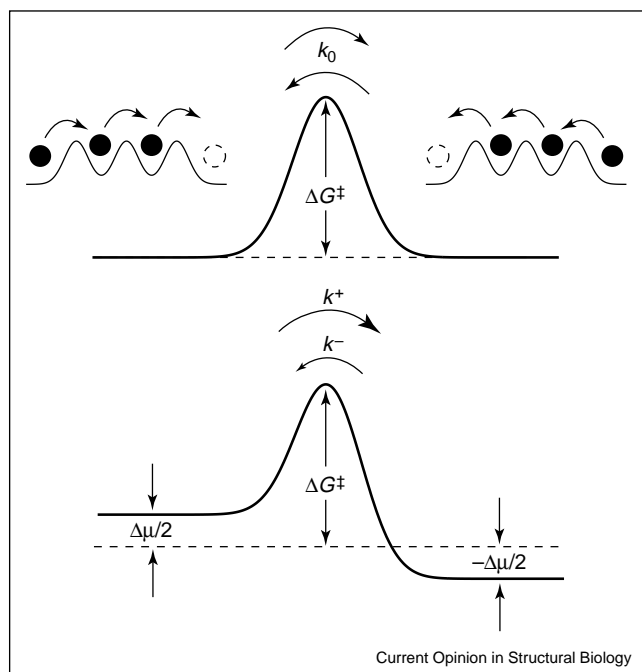
Calculating water permeability coefficients

The simulations offered the chance to address aquaporin function in quantitative terms. Calculation of permeability coefficients and comparison to measured values [3,31] provided a very sensitive test of the simulations. One additional hydrogen bond, for example, would change the permeability by two or three orders of magnitude. Apart from more qualitative treatments [26,27], two simulation approaches have mainly been followed. First, Kramers-type calculations [32[•],33[•]] were used to derive permeability coefficients from the fluctuations observed in equilibrium simulations. Second, hydrostatic or osmotic

pressures have been applied in non-equilibrium simulations, which allowed the direct observation of net water flux [34[•],35[•]].

The equilibrium approach rests on the notion that equilibrium fluctuations are closely connected to transport properties. Figure 3 explains how this relationship has now been revisited from a quite different direction [32[•]] (for a detailed treatment, see [33[•]]). Overall, remarkable agreement between simulations from different groups as well as with measured permeabilities has been obtained, which convincingly demonstrates the accuracy of the simulations. For example, the water permeability calculated from equilibrium fluctuations ($p_f = 7.5 \times 10^{-14} \text{ cm}^3/\text{s}$ [22^{**}]) is very close to the measured coefficient ($p_f = 5.43 \times 10^{-14} \text{ cm}^3/\text{s}$ [3]) for AQP1. In fact, the difference in rate coefficient of only 30% means that the activation energy was determined from the simulations to an accuracy better than $1/3 k_B T$ or 0.2 kcal/mol. That this agreement is not just anecdotal is demonstrated by suggested mutations for which permeability changes have been well reproduced by simulations [23^{**}].

Figure 3



Permeabilities (p_f) can be derived from fluctuations observed in equilibrium simulations. The appropriate collective reaction coordinate involves the motion of all water molecules that form a column within the channel. Barrier crossings (height ΔG^\ddagger) along this reaction coordinate describe the effective transport of one water molecule from one side of the channel to the other (insets top left and right). In equilibrium simulations (top), and according to Kramers' theory, forward and backward rate coefficients are equal, $k_0 = \omega_0 \exp(-\Delta G^\ddagger/k_B T)$, and no net transport occurs. Here, ω_0 is the Kramers' pre-factor ('attempt rate') and $k_B T$ is the thermal energy. In non-equilibrium simulations (bottom), the chemical potential difference ($\Delta\mu$) increases the forward rate coefficient (k^+) by a factor of $\exp(\Delta\mu/k_B T)$ with respect to the backward rate coefficient (k^-). The resulting net flux is $j = k^+ - k^- = 2k_0 \sinh(\Delta\mu/2k_B T)$ molecules per second; in linear approximation, $j = k_0 \Delta\mu/k_B T$ and $p_f = V_{\text{mol}} k_0$, where $V_{\text{mol}} \approx 30 \text{ \AA}^3$ is the volume occupied by one water molecule [32*].

Along the second route, osmotic [35*] and hydrostatic [34*] pressure gradients have been applied. Here, the *net transport* of water molecules as a result of applied pressure is directly monitored, as is the permeability. Conceptually, this is certainly a more direct approach to the situation *in vivo* and *in vitro*. On the other hand, for a non-equilibrium simulation with an applied pressure difference of one bar, a microsecond simulation would be required to see the *net transport* of only three water molecules; this would still be difficult to detect against the huge background of approximately 10 000 equilibrium barrier crossings.

For the equilibrium approach, the validity of Kramers' theory, despite the good agreement with experiment, may be questioned because of the very small free energy barrier for water permeation of about $5 k_B T$ [31]. However, in this case, all barrier crossings contribute to the

statistical accuracy of the calculated permeability. For the equilibrium simulation of, for example, AQP1, a total of approximately $n = 200$ barrier crossings were observed for the tetramer within 10 ns simulation time [22**], implying a small statistical error of $1/\sqrt{n} \approx 7\%$.

Water permeation under physiological conditions, therefore, is the result of just a tiny imbalance between forward and backward equilibrium fluctuations, which are three to four orders of magnitude more frequent than the net permeation rate. Thus, whereas the equilibrium fluctuations can be seen directly in MD simulations, extremely high hydrostatic pressures (e.g. 2000–4000 bar [34*]) are required for non-equilibrium simulations. Despite these extreme conditions, quantitative agreement with the measured permeabilities was obtained [33*]. The similarly good agreement between these two quite different simulation approaches is remarkable and suggests that both approaches, with their complementary advantages and disadvantages, can yield reliable results.

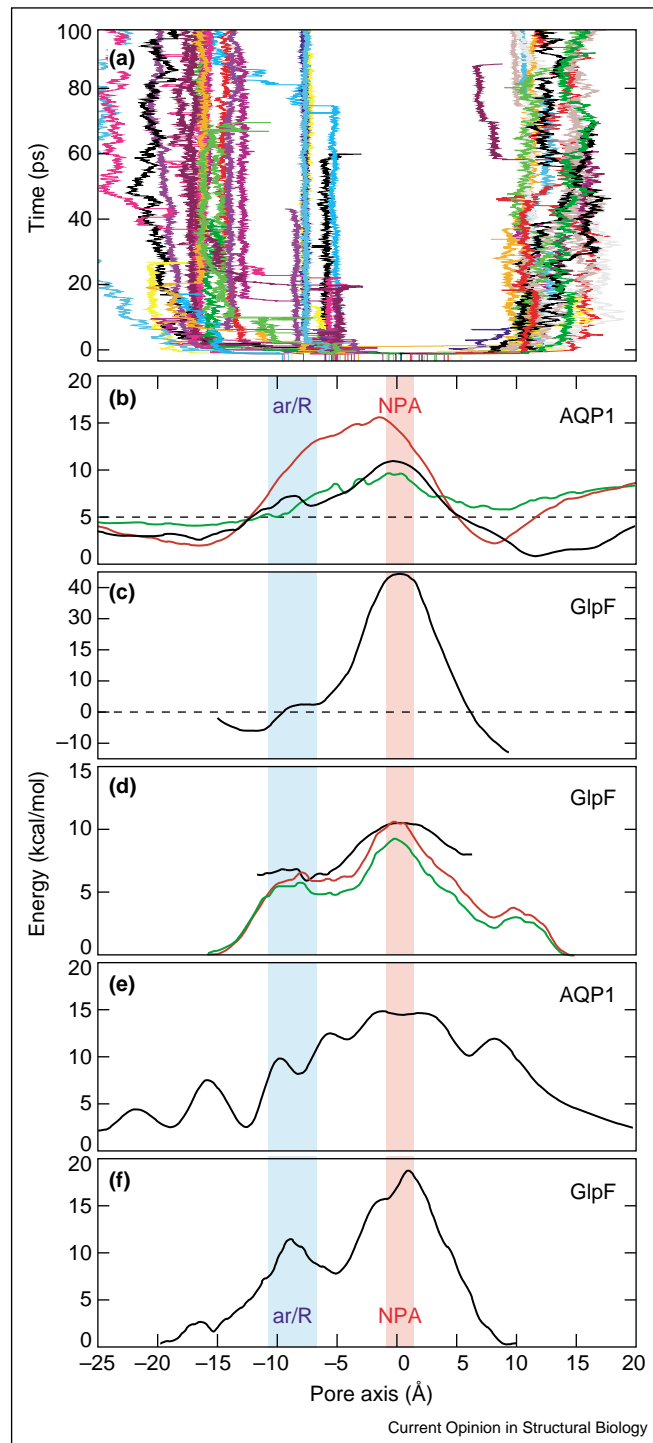
Proton exclusion

Proton conduction in bulk water proceeds via the Grotthuss mechanism. Accordingly, protons are transferred between water molecules via hydrogen bonds and transient hydronium ions. Necessarily, the water dipoles reorient during this process. The observation of interrupted hydrogen bonds along the water chain inside the pore [22**], as well as the strict orientation of the water molecules [22**,23**], led to speculation that these effects interfere with the Grotthuss mechanism and thus preclude proton conduction through the channel. Because these 'first-generation' studies were mainly aimed at — and succeeded in — explaining efficient water permeation, only (neutral) water molecules were considered and, hence, the above-mentioned speculation about the mechanism of proton exclusion was based on *indirect* evidence only.

To obtain *direct* information, explicit treatments of excess protons and proton transfer reactions in 'second-generation' simulations were considered mandatory. Several groups have accepted the challenge to address proton exclusion in aquaporins by computational methods. This has become a very active field indeed, as testified by the seven extensive simulation studies that have been published within one year [27,36**,37**,38*,39*,40,41**]. In the following, we will describe the consensus that emerges from these quite different approaches, but also discuss the discrepancies that still persist.

In a first set of 'Q-HOP' simulations [36**], protons were placed at different positions within the channel. Unexpectedly, remarkably high proton mobility through efficient Grotthuss transfers was seen throughout the channel, without any severe interruption. Furthermore, these protons were expelled from the pore within only a few picoseconds [36**] (c.f. Figure 4a). These results

Figure 4



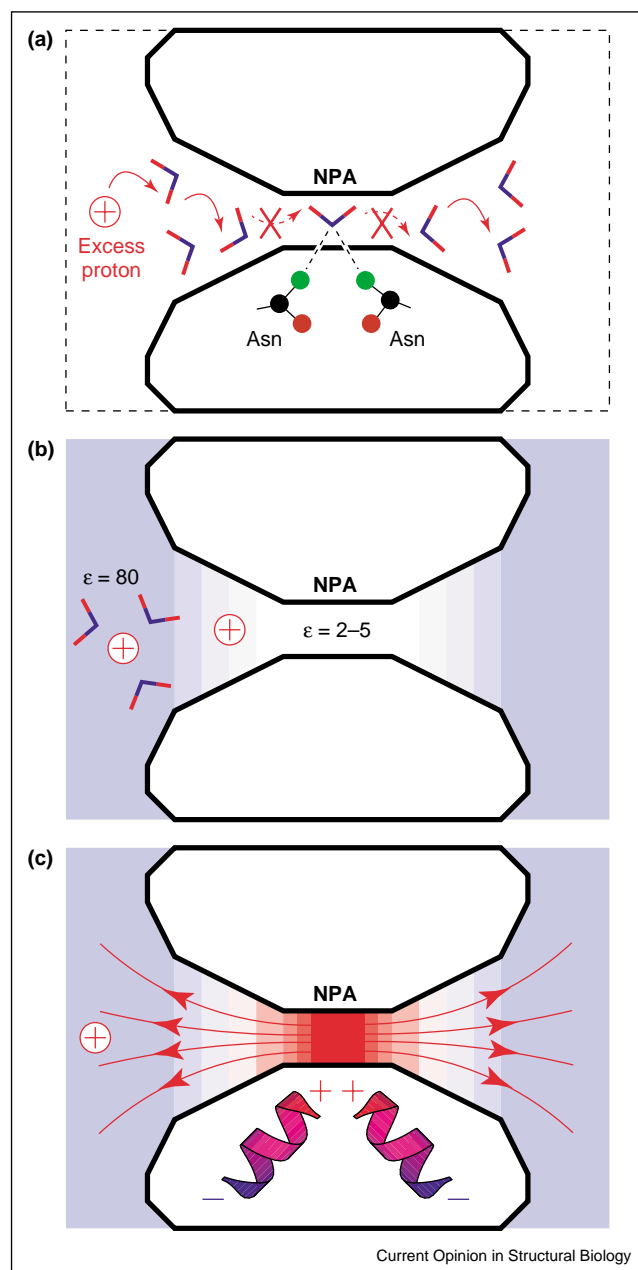
Protons are excluded from the central region of the aquaporin channel by a strong free energy barrier, as demonstrated by (a) spontaneous downhill proton trajectories from multiple Q-HOP MD simulations that started with an excess proton placed inside the channel at different positions [36**]. (b–f) Proton free energy and electrostatic profiles for the AQP1 and GlpF pores derived from various computational approaches: (b) non-equilibrium free energy profile [36**] derived from Q-HOP proton trajectories by a maximum-likelihood approach (black), electrostatic potential of mean force from MD simulations (red), energy profile from Poisson–Boltzmann calculations (green) for AQP1; (c) electrostatic potential from MD simulations of GlpF (black curve) [27]; (d) electrostatic potential (red/green) and free energy profile (black) for protons in GlpF [37**]; (e) PDL/S-LRA free energy profile for protons within the AQP1 pore (continuous line) [38**]; (f) potential of mean force for protons within the GlpF channel from EVB simulations [39*].

contrast with the original picture of an interrupted proton wire. Rather, they suggest a barrier located at the NPA region as the dominant factor preventing proton transport, irrespective of the particular underlying transport mechanism [36^{••}]. Indeed, it was found that a strong electrostatic field spans the aquaporin pore [27,36^{••}] and dominates the free energy profile for proton conduction [36^{••},37^{••},41^{••}] (c.f. Figure 4b). These findings stress the importance of simulating the explicit dynamics and energetics of protons to elucidate the proton blockage mechanism; to settle for *indirect* evidence (e.g. from structural information only or from simulations without excess protons explicitly considered) is risky.

Figure 4b–f compares the free energy and electrostatic profiles that have been obtained from the different simulation studies. The applied methods are quite diverse, including classical electrostatics calculations [27,36^{••}, 37^{••}], Q-HOP proton transfer simulations [36^{••}], semi-microscopic protein-dipole Langevin-dipole linear response approximation (PDL/D/S-LRA) calculations [38[•]], umbrella MD simulations employing the PM6 dissociable water model [37^{••},41^{••}] and steered empirical valence bond (EVB) proton transfer simulations [39[•]]. Furthermore, the profiles were calculated for two different members of the aquaporin family, AQP1 and GlpF. The quantitative differences in the barrier heights reflect the effects of the assumptions underlying the different methods and the different simulated systems. Overall, the accurate calculation of ionic barrier heights for membrane channels must be considered a challenging task even for modern simulation techniques. Nevertheless, the qualitative match between the profiles, with a clear maximum near the NPA region in the central channel and a secondary peak near the ar/R or selectivity filter region, illustrates that state-of-the-art proton transfer simulations capture the dynamics and energetics of proton transfer processes in biological systems.

The consensus conclusion is that electrostatic interactions, rather than proton wire interruption effects, are the dominant mechanism of proton exclusion in aquaporins. Surprisingly, however, a significant discrepancy concerning the nature of the electrostatic barrier persisted until very recently. Some groups claimed that proton flux is blocked by the inability of the bipolar water orientation — caused by the electrostatic field of the protein — to support the Grothuss mechanism within the NPA region [23^{••},27,39[•]]. Another group has argued that rather unspecific electrostatic desolvation effects dominate proton exclusion [38[•],40,42]. The interpretation of the findings that currently is shared by most groups attributes the proton barrier *directly* to the electrostatic field generated by the protein matrix within the NPA region; thus, this is considered the dominant factor in proton exclusion [36^{••},37^{••},41^{••}]. Accordingly, any perturbation of the proton wire at the top of the high energy barrier within

Figure 5



Schematic representation of the three mechanisms that have been proposed to dominate proton exclusion in aquaporins on the basis of simulation results. **(a)** The observed bipolar water orientation, with a central water molecule prevented from forming hydrogen bonds with neighboring water molecules, interrupts proton flux through the pore [14[•],23^{••},27]. **(b)** Unspecific desolvation effects form the main barrier to protons within the hydrophobic aquaporin pore [38[•],40,42]. **(c)** An electrostatic barrier, generated mainly by the helical macrodipoles of helices B and E and positioned at the central NPA region of the pore, is the predominant and direct determinant of proton exclusion [36^{••},37^{••},41^{••}].

the aquaporin pore would have virtually no effect, because the protons could not ‘climb’ the barrier top even if the wire was perfectly intact. We note that this

distinguishes the situation from proton conduction in bulk water, which is not impeded by larger barriers and, therefore, is directly affected by any interference with the Grotthuss mechanism [38*].

The bipolar water orientation interpretation [23**,27] (Figure 5a) rests on the observation of frequent configurations of water molecules in the pore with the oxygen atom of a central water molecule saturated with hydrogen bonds to the sidechains of the two asparagines of the NPA motifs. This was proposed to prohibit the acceptance of an excess proton at this position, thereby interrupting proton flux through the pore [23**,27]. This elegant proposal is similar in spirit to the speculation based on the first atomic model of the structure of AQP1 [14*]. This proposal rests on the assumption that proton exclusion is caused by interruption of a Grotthuss-type proton wire and that the orientational restriction of water molecules in the pore causes such an interruption. However, simulations that explicitly include proton transfer reactions within the pore are not compatible with this assumption. In contrast to the proposed mechanism, proton transfer within the NPA region was found not to be impeded, suggesting that orientational restriction of water molecules is not the dominant determinant of proton exclusion from the aquaporin pore [36**,37**,41**].

Likewise, the proposed mechanism of proton exclusion by a non-specific desolvation barrier [38*,40,42] (Figure 5b) seems incompatible with several findings. This mechanism predicts that the central barrier near the NPA region is caused by the geometry and hydrophobicity of the pore, rather than by the electrostatic field in the channel, which is generated by the arrangement of charged and polar groups lining the pore. Indeed, the authors show that very similar free energy profiles are obtained for protons moving through the AQP1 pore and a hydrophobic model channel [38*].

However, in a recent study, in which the effect of the protein's charged and polar groups was investigated by switching off the partial charges of the NPA motifs and the B and E helical macrodipoles, the proton transfer barrier was shown to be drastically reduced [41**]. This finding supports the proposed mechanism of a direct electrostatic barrier [36**,37**] generated by the protein matrix (Figure 5c). This interpretation renders the bipolar water orientation a secondary effect rather than the primary cause of proton exclusion — a picture that is also consistent with all other simulation results. Furthermore, mutants have been suggested [41**] that could cause proton leakage, thus providing an experimental test of this proposed mechanism.

Conclusions

Taken together, these findings show that electrostatic effects dominate the mechanism of proton exclusion in

aquaporins. At the same time, the different interpretations once again underscore the challenge of unraveling the underlying structural and energetic determinants of the remarkable functional duality of the aquaporin family of proteins: efficient water/solute permeation while strictly blocking proton flux.

Acknowledgements

We thank Andreas Engel, Volkhard Helms, Régis Pomès, Jochen Hub and Peter Pohl for carefully reading the manuscript and for stimulating discussions. This work was supported by the BIOTECH program of the European Union (grants QLRT-2000/00778 and QLRT-2000/00504).

References and recommended reading

Papers of particular interest, published within the annual period of review, have been highlighted as:

- of special interest
 - of outstanding interest
1. Preston GM, Carroll TP, Guggino WB, Agre P: **Appearance of water channels in *Xenopus* oocytes expressing red-cell CHIP28 protein.** *Science* 1992, **256**:385-387.
 2. Agre P, Bonhivers M, Borgnia MJ: **The aquaporins, blueprints for cellular plumbing systems.** *J Biol Chem* 1998, **273**:14659-14662.
 3. Engel A, Stahlberg H: **Aquaglyceroporins: channel proteins with a conserved core, multiple functions and variable surfaces.** *Int Rev Cytol* 2002, **215**:75-104.
 4. King LS, Kozono D, Agre P: **From structure to disease: the evolving tale of aquaporin biology.** *Nat Rev Mol Cell Biol* 2004, **5**:687-698.
 5. Mitchell P: **Coupling of phosphorylation to electron and hydrogen transfer by a chemi-osmotic type of mechanism.** *Nature* 1961, **191**:144-148.
 6. Zeidel ML, Nielsen S, Smith BL, Ambudkar SV, Maunsbach AB, Agre P: **Ultrastructure, pharmacological inhibition, and transport selectivity of aquaporin channel-forming integral protein in proteoliposomes.** *Biochemistry* 1994, **33**:1606-1615.
 7. Marx D, Tuckerman ME, Hutter J, Parrinello M: **The nature of the hydrated excess proton in water.** *Nature* 1999, **397**:601-604.
 8. Schmitt UW, Voth GA: **The computer simulation of proton transport in water.** *J Chem Phys* 1999, **111**:9361-9381.
 9. Akeson M, Deamer DW: **Proton conductance by the gramicidin water wire.** *Biophys J* 1991, **60**:101-109.
 10. Pomès R, Roux B: **Structure and dynamics of a proton wire: a theoretical study of H⁺ translocation along the single-file water chain in the gramicidin A channel.** *Biophys J* 1996, **71**:19-39.
 - See annotation to [11*].
 11. Pomès R, Roux B: **Free energy profiles for H⁺ conduction along hydrogen-bonded chains of water molecules.** *Biophys J* 1998, **75**:33-40.
 - Two papers [10*,11*] describe the first explicit simulation study of proton conduction and energetics within a membrane channel.
 12. Kandori H, Yamazaki Y, Sasaki J, Needleman R, Lanyi JK, Maeda A: **Water-mediated proton-transfer in proteins - an FTIR study of bacteriorhodopsin.** *J Am Chem Soc* 1995, **117**:2118-2119.
 13. Baudry J, Tajkhorshid E, Molnar F, Phillips J, Schulten K: **MD study of bacteriorhodopsin and the purple membrane.** *J Phys Chem B* 2001, **105**:905-918.
 14. Murata K, Mitsuoka K, Walz T, Agre P, Heymann J, Engel A, Fujiyoshi Y: **Structural determinants of water permeation through aquaporin-1.** *Nature* 2000, **407**:599-605.
 - The first atomic model of AQP1, derived from cryo-electron crystallography data. The authors propose that strong hydrogen bonds between water molecules located at the center of the pore and the NPA region interrupt the Grotthuss proton wire and thereby block proton conduction.

15. Fu D, Libson A, Miercke LJ, Weitzman C, Nollert P, Krucinski J, Stroud RM: **Structure of a glycerol-conducting channel and the basis for its selectivity.** *Science* 2000, **290**:481-486.
This first high-resolution structure of the bacterial glyceroporin GlpF provided the basis for several of the MD simulations discussed within this review.
16. Fujiyoshi Y, Mitsuoka K, de Groot BL, Philippsen A, Grubmüller H, Agre P, Engel A: **Structure and function of water channels.** *Curr Opin Struct Biol* 2002, **12**:509-515.
17. Werten P, Rémy HW, de Groot BL, Fotiadis D, Philippsen A, Stahlberg H, Grubmüller H, Engel A: **Progress in the analysis of membrane protein structure and function.** *FEBS Lett* 2002, **529**:65-72.
18. de Groot BL, Engel A, Grubmüller H: **The structure of the aquaporin-1 water channel: a comparison between cryo-electron microscopy and X-ray crystallography.** *J Mol Biol* 2003, **325**:485-493.
19. Stroud RM, Savage D, Miercke LJW, Lee JK, Khademi S, Harries W: **Selectivity and conductance among the glycerol and water conducting aquaporin family of channels.** *FEBS Lett* 2003, **555**:79-82.
20. de Groot BL, Engel A, Grubmüller H: **A refined structure of human aquaporin-1.** *FEBS Lett* 2001, **504**:206-211.
21. Sui H, Han B-G, Lee JK, Walian P, Jap BK: **Structural basis of water-specific transport through the AQP1 water channel.** *Nature* 2001, **414**:872-878.
This X-ray structure of AQP1 confirmed the refined AQP1 model that had been derived by cryo-electron crystallography.
22. de Groot BL, Grubmüller H: **Water permeation across biological membranes: mechanism and dynamics of aquaporin-1 and GlpF.** *Science* 2001, **294**:2353-2357.
The authors describe MD simulations of spontaneous water permeation through fully solvated AQP1 and GlpF embedded within a lipid bilayer. Agreement with experimental water permeation rates is obtained and a detailed mechanism for efficient water permeation proposed. The strong orientation of water dipoles and interruption of hydrogen bonds along the proton wire are observed. The authors speculate that proton blockage is related to these effects.
23. Tajkhorshid E, Nollert P, Jensen MØ, Miercke LJW, O'Connell J, Stroud RM, Schulten K: **Control of the selectivity of the aquaporin water channel family by global orientational tuning.** *Science* 2002, **296**:525-530.
A glycerol-free X-ray structure of GlpF is presented. MD simulations of a fully solvated tetramer within a lipid bilayer confirmed the strong orientation of water molecules within the pore. The electrostatic field generated by helices B and E are identified as the main cause of the orientational preference, which is proposed to be the dominant mechanism of proton selectivity. Mutations that affect water permeation are suggested and explained through simulations.
24. Jung JS, Preston GM, Smith BL, Guggino WB, Agre P: **Molecular structure of the water channel through aquaporin CHIP - the hourglass model.** *J Biol Chem* 1994, **269**:14648-14654.
25. Heymann JB, Engel A: **Structural clues in the sequences of the aquaporins.** *J Mol Biol* 2000, **295**:1039-1053.
26. Vidossich P, Cascella M, Carloni P: **Dynamics and energetics of water permeation through the aquaporin channel.** *Proteins* 2004, **55**:924-931.
27. Jensen MØ, Tajkhorshid E, Schulten K: **Electrostatic tuning of permeation and selectivity in aquaporin water channels.** *Biophys J* 2003, **85**:2884-2899.
28. Jensen MØ, Tajkhorshid E, Schulten K: **The mechanism of glycerol conduction in aquaglyceroporins.** *Structure* 2001, **9**:1083-1093.
29. Jensen MØ, Park S, Tajkhorshid E, Schulten K: **Energetics of glycerol conduction through aquaglyceroporin GlpF.** *Proc Natl Acad Sci USA* 2002, **99**:6731-6736.
The first calculation of the free energy profile for glycerol conduction through GlpF from multiple steered MD using Jarzynski's equation.
30. Lu D, Grayson P, Schulten K: **Glycerol conductance and physical asymmetry of the Escherichia coli glycerol facilitator GlpF.** *Biophys J* 2003, **85**:2977-2987.
31. Borgnia MJ, Agre P: **Reconstitution and functional comparison of purified GlpF and AqpZ, the glycerol and water channels from Escherichia coli.** *Proc Natl Acad Sci USA* 2001, **98**:2888-2893.
32. de Groot BL, Tieleman DP, Pohl P, Grubmüller H: **Water permeation through gramicidin A: desformylation and the double helix; a molecular dynamics study.** *Biophys J* 2002, **82**:2934-2942.
A theory to calculate non-equilibrium water permeation coefficients from the stochastic fluctuations of water molecules in equilibrium simulations of nanoscale water channels is proposed. The theory is applied to calculate osmotic permeation coefficients from equilibrium simulations of water permeation through gramicidin A.
33. Zhu FQ, Tajkhorshid E, Schulten K: **Theory and simulation of water permeation in aquaporin-1.** *Biophys J* 2004, **86**:50-57.
A carefully presented didactic compendium of the theory for calculating non-equilibrium water permeation coefficients from equilibrium simulations. The theory is applied to AQP1 and agreement with measured permeability coefficients is obtained.
34. Zhu F, Tajkhorshid E, Schulten K: **Pressure-induced water transport in membrane channels studied by molecular dynamics.** *Biophys J* 2002, **83**:154-160.
The first attempt to induce water flux through aquaporins by hydrostatic pressure. Despite the high pressures needed to observe significant water flux, agreement with measured rates is obtained for GlpF.
35. Kalra A, Garde S, Hummer G: **Osmotic water transport through carbon nanotube membranes.** *Proc Natl Acad Sci USA* 2003, **100**:10175-10180.
This first direct simulation of osmotically driven water flux through a nanopore provides a microscopic picture of the stochastic nature of the nanoscale flows. The observed transient water structures render continuum treatments problematic.
36. de Groot BL, Frigato T, Helms V, Grubmüller H: **The mechanism of proton exclusion in the aquaporin-1 water channel.** *J Mol Biol* 2003, **333**:279-293.
The first simulation of explicit proton dynamics within the AQP1 pore. It is shown that the Grothuss mechanism is fully intact throughout the pore, and that protons and hydronium ions are excluded from the pore by a free energy barrier that is dominated by electrostatic forces. Also, hydroxide ions are seen to be blocked by an energy barrier. The water orientation is suggested to be an electrostatic side-effect, rather than the cause of proton selectivity.
37. Chakrabarti N, Tajkhorshid E, Roux B, Pomes R: **Molecular basis of proton blockage in aquaporins.** *Structure* 2004, **12**:65-74.
The authors calculated the free energy barrier blocking proton conduction through GlpF using umbrella sampling simulations with a dissociable water model. The study corroborates [36**] in that the barrier is dominated by electrostatic forces. The energy needed to reorient the water dipoles against the strong fields is calculated.
38. Burykin A, Warshel A: **What really prevents proton transport through aquaporin? Charge self-energy versus proton wire proposals.** *Biophys J* 2003, **85**:3696-3706.
Unspecific desolvation effects are proposed as the dominant cause of proton selectivity in aquaporins; however, this seems incompatible with the results presented in [37**].
39. Ilan B, Tajkhorshid E, Schulten K, Voth GA: **The mechanism of proton exclusion in aquaporin channels.** *Proteins* 2004, **55**:223-228.
Free energy calculations using a multistate EVB model of proton conduction are presented. This independent description of proton transfer reactions confirmed the location and shape of the main barrier to proton conduction, as well as the existence of a secondary barrier at the restriction region.
40. Burykin A, Warshel A: **On the origin of the electrostatic barrier for proton transport in aquaporin.** *FEBS Lett* 2004, **570**:41-46.
41. Chakrabarti N, Roux B, Pomes R: **Structural determinants of proton blockage in aquaporins.** *J Mol Biol* 2004, **343**:493-510.
Employing the methods established in [37**], it is convincingly shown that the free energy barrier is dominated by the helix B and E macrodipoles. Desolvation effects are shown not to contribute significantly to the main barrier, but rather cause a penalty at the pore entry regions. It is also shown that the bipolar orientation of the water chain does not in itself oppose proton translocation. A single mutant that could leak protons is suggested.
42. Eisenberg B: **Why can't protons move through water channels?** *Biophys J* 2003, **85**:3427-3428.